

Polymerization of α -Amino Acid *N*-Carboxyanhydrides Catalyzed by Rare Earth Tris(borohydride) Complexes: Mechanism and Hydroxy-Endcapped Polypeptides

Hui Peng,¹ Jun Ling,¹ Yinghong Zhu,² Lixin You,¹ Zhiqian Shen¹

¹Department of Polymer Science and Engineering, MOE Key Laboratory of Macromolecular Synthesis and Functionalization, Zhejiang University, Hangzhou 310027, People's Republic of China

²College of Chemical Engineering and Materials, Zhejiang University of Technology, Hangzhou 310014, People's Republic of China

Correspondence to: J. Ling (E-mail: lingjun@zju.edu.cn)

Received 13 January 2012; accepted 21 March 2012; published online

DOI: 10.1002/pola.26077

ABSTRACT: In this work, rare earth tris(borohydride) complexes, $\text{Ln}(\text{BH}_4)_3(\text{THF})_3$ ($\text{Ln} = \text{Sc}, \text{Y}, \text{La}, \text{and Dy}$), have been used to catalyze the ring-opening polymerization of γ -benzyl-L-glutamate *N*-carboxyanhydride (BLG NCA). All the catalysts show high activities and the resulting poly(γ -benzyl-L-glutamate)s (PBLGs) are recovered with high yields ($\geq 90\%$). The molecular weights (MWs) of PBLG can be controlled by the molar ratios of monomer to catalyst, and the MW distributions (MWDs) are relatively narrow (as low as 1.16) depending on the rare earth metals and reaction temperatures. Block copolypeptides can be easily synthesized by the sequential addition of two monomers. The obtained P(γ -benzyl-L-glutamate-*b- ϵ* -carbobenzoxy-L-lysine) [P(BLG-*b*-BLL)] and P(γ -benzyl-L-glutamate-*b*-alanine) [P(BLG-*b*-ALA)] have been well characterized by NMR, gel permeation chromatography, and differential scanning calorimetry measurements. A random copolymer P(BLG-*co*-BLL) with a narrow MWD of 1.07 has also been synthesized. The polymerization mechanisms have been investigated in detail. The results show that both nucleo-

philic attack at the 5-CO of NCA and deprotonation of 3-NH of NCA in the initiation process take place simultaneously, resulting in two active centers, that is, an yttrium ALA carbamate derivative [$\text{H}_2\text{BOCH}_2(\text{CH})\text{NHC}(\text{O})\text{OLn}-$] and a *N*-yttrium-lated ALA NCA. Propagation then proceeds on these centers via both normal monomer insertion and polycondensation. After termination, two kinds of telechelic polypeptide chains, that is, α -hydroxyl- ω -aminotelechelic chains and α -carboxylic- ω -aminotelechelic ones, are formed as characterized by MALDI-TOF MS, ^1H NMR, ^{13}C NMR, ^1H - ^1H COSY, and ^1H - ^{13}C HMQC measurements. By decreasing the reaction temperature, the normal monomer insertion pathway can be exclusively selected, forming an unprecedented α -hydroxyl- ω -aminotelechelic polypeptide. © 2012 Wiley Periodicals, Inc. *J Polym Sci Part A: Polym Chem* 000: 000–000, 2012

KEYWORDS: α -amino acid *N*-carboxyanhydride; biopolymers; catalysts; polypeptides; rare earth catalysts; ring-opening polymerization

INTRODUCTION Polypeptides are a class of important biomaterials in drug delivery,^{1,2} tissue engineering,³ and nanoscale self-assembly.⁴ The most important method for polypeptide synthesis is the ring-opening polymerization (ROP) of amino acid *N*-carboxyanhydrides (NCAs).⁵ After the discovery of NCA monomers by Leuchs, catalysts used to polymerize them have been received great attention.^{6,7} They are mainly categorized into three classes. (1) Amines (primary amines, secondary amines, and tertiary amines), alcohols, thiols,⁸ and water are metal-free catalysts among which primary and tertiary amines are the most widely used, so far, for their easily accessible reasons. In general, primary amine is good for preparing low-molecular weight (MW) polypeptides with the MWs close to the theoretical ones. Tertiary amine, in the

contrary, produces soluble polypeptides with extremely high MWs.⁹ The MW distributions (MWDs) are reported as broad as 2.8¹⁰ and even bimodal.¹¹ (2) Metal salts and organometallic compounds are another class of catalysts. During the past few years, some metallic compounds were developed for ROP of NCA, for instance, solution of lithium chloride in *N,N*-dimethylformamide (DMF), sodium carbamate, 9-fluorenyl potassium, sodium hydride, sodium acetate, sodium methoxide, diethylzinc, tributylaluminum, diethylcadmium, and tributyltinmethoxide.^{6,9} These polymerizations, however, were plagued by a variety of side reactions which resulted in the uncontrolled MWs and broad MWDs. (3) Zero-valent nickel complex bipyNi(COD) (bipy = 2,2'-bipyridyl, COD = 1,5-cyclooctadiene) reported by Deming realized living

Additional Supporting Information may be found in the online version of this article.

© 2012 Wiley Periodicals, Inc.

polymerization of NCAs and facile block polypeptide synthesis.^{12,13} In 2007, Cheng and coworkers^{11,14,15} used hexamethyldisilazane and its derivatives as the initiators for controlled polymerization of NCAs. The MWs of polypeptides obtained were found to be close to calculated values and MWDs were narrow. Recently, some methods have been reported to improve the primary amine systems, including high-vacuum techniques,^{16–18} decreasing the reaction temperature^{19–21} and pressure,²² and treating the primary amine with hydrochloride.²³ Besides exploring new catalysts, great progress has also been made on the mechanisms of NCA polymerization by Kricheldorf et al.,^{24–26} Messman and coworkers,²⁷ and our group²⁸ with some aspects still unclear.

The organometallic catalysts for ROP of NCA are mainly focused on alkali-, alkaline-earth-, and late-transition metals. Rare earth metal compounds are nearly unexplored in polypeptide synthesis while they are well-known catalysts in ROP of lactones, lactides, and cyclic carbonates.^{29–36} To the best of our knowledge, only one paper reported the polymerization of γ -stearyl-L-glutamate NCA initiated by rare earth catalyst. Triple component catalytic system of neodymium acetylacetonate [Nd(acac)₃] or neodymium tris(2-ethylhexylphosphonate) [Nd(P₂₀₄)₃] together with triethylaluminum and water produced high-MW polyglutamates with relatively narrow MWDs.³⁷ As organometallic catalyst has its advantages over the conventional catalytic systems on the propagating chain-end control,^{5,10} and rare earth compound shows a promising result to NCA polymerization, we performed the study of ROP of NCAs by rare earth metallic catalysts.

In this article, we report rare earth tris(borohydride) [Ln(BH₄)₃(THF)₃] complex as the first homogeneous single-component catalyst to polymerize NCAs. The strong coordination ability of rare earth metals and the reductivity of the ligand with the rare earth metal-borohydride hydrogen bond (Ln-HBH₃) are of our interest in NCA polymerization. Polymerization features were presented and polymerization mechanism was detailedly studied. Further, based on this mechanism, a strategy to synthesize an unprecedented α -hydroxyl- ω -aminotelechelic polypeptide was developed.

EXPERIMENTAL

Materials

γ -Benzyl-L-glutamate (BLG) (99.0%, Shanghai Hanhong Chemical, China), ϵ -carbobenzoxy-L-lysine (BLL) (98.5%, Shanghai Hanhong Chemical), L-alanine (ALA) (98.5%, Sino-pharm Chemical Reagent, China), and sodium borohydride (96.0%, Sino-pharm Chemical Reagent) were used as received. Tetrahydrofuran (THF) and hexane were refluxed over potassium/benzophenone ketyl before use. Ethyl acetate was stirred over CaH₂ and distilled. DMF was purified by drying over 4 Å molecular sieves followed by vacuum distillation. Dimethyl sulfoxide (DMSO) was stirred over CaH₂ and vacuum distilled.

Synthesis of BLG NCA, BLL NCA, and ALA NCA

In a typical procedure, BLG (10.1 g, 42.2 mmol) was charged into a 250 mL round bottom Schlenk flask followed by add-

ing 100 mL anhydrous THF under argon. Triphosgene (4.60 g, 15.5 mmol), dissolved in 20 mL anhydrous THF, was added dropwise into the BLG/THF solution during 30 min. The reaction was left to proceed for a further 2 h under argon atmosphere until a clear solution was obtained. The solution was concentrated and poured into anhydrous hexane. The crude white precipitate was purified by recrystallization four times using a mixture of ethyl acetate and hexane resulting in BLG NCA in crystalline form (10.37 g, 83%).

¹H NMR (CDCl₃, 500 MHz): δ = 7.3–7.4 (m, 5H, ArH), 6.72 (s, 1H, NH), 5.13 (s, 2H, C₆H₅CH₂–), 4.38 (dd, 1H, α -CH), 2.58 (t, 2H, β -CH₂), 2.27 (m, 1H, γ -CH), and 2.11 (m, 1H, γ -CH).

The BLL NCA (76%) and ALA NCA (53%) were synthesized following similar procedures. BLL ¹H NMR (CDCl₃, 500 MHz): δ = 7.3–7.4 (m, 5H, ArH), 7.01 (s, 1H, ring NH), 5.10 (s, 2H, C₆H₅CH₂–), 4.96 (s, 1H, side chain NH), 4.26 (dd, 1H, α -CH), 3.20 (m, 2H, NCH₂), 1.80–1.95 (m, 2H, β -CH), and 1.56–1.40 (m, 4H, –NHCH₂CH₂CH₂CH₂–). ALA ¹H NMR (CDCl₃, 500 MHz): δ = 6.30 (s, 1H, NH), 4.42 (q, 1H, –CH), and 1.58 (d, 3H, –CH₃).

Synthesis of the Catalysts Ln(BH₄)₃(THF)₃

Ln(BH₄)₃(THF)₃ (Ln = Sc, Y, La, and Dy) were prepared using literature procedures²⁹ and our previous report.³⁸ For example, YCl₃ (1.040 g, 5.3 mmol), NaBH₄ (0.643 g, 16.9 mmol), and THF (50 mL) were mixed and the suspension was allowed to stir at 60 °C for 48 h. After centrifugation separation, the liquid was allowed to crystallize and dried in dynamic vacuum (yield = 63%).

¹H NMR (CDCl₃, 400 MHz): δ = 4.06 (t, 12H, –OCH₂–), 1.97 (m, 12H, –OCH₂CH₂–), and 0.55 (q, 12H, –BH₄).

Polymerization of BLG NCA

All polymerizations were performed in Schlenk tubes under argon. In a typical polymerization, a mixture of BLG NCA (0.418 g, 1.59 mmol) in 3 mL DMF and 0.30 mL Y(BH₄)₃(THF)₃ (0.1034 mol/L in THF) was sealed in a tube and placed in a 40 °C thermostated oil bath for 24 h. The produced polymer was isolated by precipitation from methanol containing 5% HCl, washed with methanol, and dried in vacuum (yield = 87.6%).

Polymerization of ALA NCA

In a typical polymerization, ALA NCA (0.204 g, 1.77 mmol) was first dissolved in 2 mL THF; 0.20 mL Y(BH₄)₃(THF)₃ (0.0860 mol/L in THF) was then added by syringe. The tube was sealed and placed at room temperature for 3 days. The produced polymer was isolated by precipitation from diethyl ether (yield >99%).

Copolymerization of NCAs

For the synthesis of random copolypeptides, BLG NCA (0.224 g, 0.852 mmol) and BLL NCA (0.151 g, 0.494 mmol) were dissolved in 4 mL DMF; 0.18 mL of Y(BH₄)₃(THF)₃ (0.0366 mol/L in THF) was then added by syringe. The tube was sealed and the reaction was performed at room temperature

TABLE 1 Polymerizations of BLG NCA Catalyzed by $\text{Ln}(\text{BH}_4)_3(\text{THF})_3$ ($\text{Ln} = \text{Sc}, \text{Y}, \text{La}, \text{and Dy}$)^a

Run	Catalyst	[M]/[Ln]	Temp. (°C)	Yield (%)	$M_{\text{theo.}}^b$ (10 ⁴ Da)	M_n^c (10 ⁴ Da)	MWD ^c
1	$\text{Y}(\text{BH}_4)_3$	51	40	87.6	0.33	2.01	1.5 ₁
2	$\text{Y}(\text{BH}_4)_3$	198	40	90.9	1.27	5.25	1.4 ₃
3	$\text{Y}(\text{BH}_4)_3$	1,163	40	92.0	7.81	8.62	1.3 ₂
4	$\text{Y}(\text{BH}_4)_3$	404	25	89.7	2.65	5.21	1.3 ₁
5	$\text{Y}(\text{BH}_4)_3$	397	0	65.5	1.90	3.09	1.1 ₈
6	$\text{Sc}(\text{BH}_4)_3$	219	40	98.0	1.57	3.51	1.6 ₅
7	$\text{La}(\text{BH}_4)_3$	206	40	89.5	1.35	4.98	1.2 ₉
8	$\text{Dy}(\text{BH}_4)_3$	175	40	90.1	1.15	5.68	1.1 ₆

^a Reaction conditions: [BLG NCA] = 0.5 mol/L, 24 h in DMF.

^b $M_{\text{theo.}} = [\text{molar mass}_{\text{BLG NCA}} - 44] \times ([\text{M}]/[\text{Ln}]/3) \times \text{yield}$.

^c Determined by GPC/MALLS in DMF containing 0.1 mol/L LiBr at 60 °C ($dn/dc = 0.104 \text{ mL/g}$).

for 36 h. The polymer was isolated by precipitation from diethyl ether (yield = 71.6%).

For the synthesis of block copolypeptides, BLG NCA (0.405 g, 1.54 mmol) was first dissolved in 3 mL DMF, and 0.20 mL $\text{Y}(\text{BH}_4)_3(\text{THF})_3$ (0.0366 mol/L in THF) was then added by syringe. The tube was sealed and the reaction was performed at room temperature for 24 h to ensure complete conversion of the monomers [monitored by Fourier transform infrared spectra (FT-IR)]. Then, 1.8 mL of the reaction mixture was withdrawn from the tube and precipitated from diethyl ether (yield = 87.2%) for the analysis of first block. BLL NCA (0.173 g, 0.565 mmol) dissolved in 1.6 mL DMF was then added to the reaction mixture and the polymerization of the second block was complete after 72 h. The product was isolated by precipitation into diethyl ether (yield = 94.8%). Block polypeptides of BLG NCA and ALA NCA were prepared in a similar way.

Reaction of ALA NCA With $\text{Y}(\text{BH}_4)_3(\text{THF})_3$

A $\text{Y}(\text{BH}_4)_3(\text{THF})_3/\text{THF}$ solution (0.0861 mol/L, 10 mL, 0.861 mmol) was stirred at room temperature. ALA NCA (0.300 g, 2.601 mmol) dissolved in 2-mL THF was then added dropwise. A white precipitate rapidly appeared in a colorless solution accompanied with gas evolution. After 1 day, the solution was filtered and the resulting white powder was washed thoroughly with THF for two times and finally dried in vacuum. The white solid (yield = 83%) was analyzed by ESI-MS, FT-IR, and ¹³C NMR.

Measurements

NMR spectra were recorded on a Bruker Avance DMX 500 spectrometer (¹H: 500 MHz, ¹³C: 125 MHz) using CDCl_3 /trifluoroacetic acid (CF_3COOH) (v:v = 3:1), CF_3COOD or $\text{DMSO}-d_6$ as solvent and tetramethylsilane, or CF_3COOH as internal reference. MWs and MWDs were determined by gel permeation chromatography/multiangle laser light scattering (GPC/MALLS) which consisted of a Waters 1515 isocratic high-performance liquid chromatograph pump, a Wyatt DAWN DSP MALLS detector, a Wyatt Optilab DSP interferometric refractometer, and two columns of Styragel (HT3 and HT4). DMF containing 0.1 mol/L LiBr was used as the eluent with a flow rate of 1.0 mL/min at 60 °C. Differential scanning calo-

rimetry (DSC) analyses were performed on a Perkin Elmer Pyris 1 instrument. Samples were heated from -50 to 150 °C at a rate of 10 °C/min under a nitrogen purge, quenched to -50 °C and subjected to a second scan. The first and second thermo-scanning curves were recorded. The MALDI-TOF mass spectra were measured on an Applied Biosystems Voyager System 4350 equipped with a nitrogen laser ($\lambda = 337 \text{ nm}$). All mass spectra were recorded in the reflection mode with an acceleration voltage of 20 kV. The irradiation targets were prepared from hexafluoroisopropyl alcohol solutions with 2,5-dihydroxybenzoic acid as matrix and potassium trifluoroacetate as dopant. ESI-MS was measured on a Varian 500 mass spectrometer. The FT-IR were recorded on a Bruker VECTOR 22 spectrometer either in Nujol mull or neat using KBr plates.

RESULTS AND DISCUSSION

Polymerization Features

The homoleptic trivalent rare earth metal borohydride complexes $\text{Ln}(\text{BH}_4)_3(\text{THF})_3$ ($\text{Ln} = \text{Sc}, \text{Y}, \text{La}, \text{and Dy}$) are efficient catalysts for ROP of BLG NCA. Table 1 summarizes the results of the polymerizations performed in DMF for 24 h. In general, the polymer poly(γ -benzyl-L-glutamate) (PBLG) was recovered in about 90% yield. The monomer was completely consumed within 24 h as proved by FT-IR and ¹H NMR. PBLG with the MWs ranging from 2×10^4 to 9×10^4 Da and relatively narrow MWDs (1.32–1.51) could be prepared by varying the molar ratios of monomer to catalyst (runs 1–3 in Table 1), in contrast to the strong-base catalyst such as triethylamine which showed no controllability to the MWs.³⁹ MWs and MWDs also depend on the reaction temperature. Low temperature inclined to produce polypeptides with low-MWs and narrow MWDs. At 0 °C (run 5 in Table 1), PBLG with MW of 31 KDa and MWD of 1.18 was obtained. However, the experimental MW is deviated from the theoretical one, this may be related to the difference of the three BH_4 ligands.²⁹ Four rare earth tris(borohydride) complexes, that is, $\text{Ln}(\text{BH}_4)_3(\text{THF})_3$, ($\text{Ln} = \text{Sc}, \text{Y}, \text{La}, \text{and Dy}$), were used as initiators of BLG NCA. At comparable monomer to catalyst molar ratios (runs 2, 6, 7, and 8 in Table 1), $\text{Sc}(\text{BH}_4)_3(\text{THF})_3$ produced PBLG with the lowest MW (3.5×10^4 Da) and the broadest MWD (MWD = 1.65). The other three catalysts

TABLE 2 Block and Random Copolymerizations of NCAs Catalyzed by $Y(BH_4)_3(THF)_3$.^a

Run	M_I/M_{II} ^b	$[M_I]/[Y]$	n_{II}/n_I (feed)	Time (day)	Yield (%)	n_{II}/n_I ^c (product)	$M_{theo.}$ (10^4 Da)	M_n^d (10^4 Da)	MWD ^d
1	BLG NCA/BLG NCA	200	1.11	1+3	95.0	–	1.39/2.93	2.19/4.41	1.3 ₀ /1.2 ₃
2	BLG NCA/BLL NCA	210	0.92	1+3	94.8	0.92	1.45/3.05	2.58/3.87	1.2 ₀ /1.1 ₄
3	BLG NCA/ALA NCA	413	0.61	1+3	89.3	0.69	–	–	–
4	BLG NCA/BLL NCA	129	0.58	1.5	71.6	0.54	0.89	2.57	1.0 ₇

BLG NCA: γ -benzyl-L-glutamate *N*-carboxyanhydrid; BLL NCA: ϵ -carboxybenzoxy-L-lysine *N*-carboxyanhydride; ALA NCA: L-alanine *N*-carboxyanhydride.

^a Reaction conditions: [BLG NCA] = 0.5 mol/L, 25 °C in DMF.

^b Feeding mode: sequential addition (runs 1–3) and simultaneous addition (run 4).

^c Calculated from 1H NMR spectra of products from the integration (Int.) ratios Int.PBLL/Int.PBLG using the methine groups (COCHRNH, δ = 4.61 ppm for PBLG and δ = 4.41 ppm for PBLL) and [Int.PALA/3]/[Int.PBLG/2] using the methyl group and benzyl group (CH_3CH , δ = 1.47 ppm for PALA and $C_6H_5CH_2$, δ = 5.07 ppm for PBLG).

^d Determined by GPC/MALLS in DMF containing 0.1 mol/L LiBr at 60 °C.

produced PBLGs with similar MWs but different MWDs ranging from 1.16 to 1.43. This result may be related to the differences of atom radius and electronic structures of rare earth metals.

Block and random copolypeptide can also be synthesized by $Y(BH_4)_3(THF)_3$ as shown in Table 2. After the first block polymerization was completed, the second batch of NCA monomer including BLG NCA, BLL NCA, and ALA NCA was added (runs 1–3 in Table 2). The products were submitted to 1H NMR (Fig. 1) and GPC (Fig. 2) analyses to test the formation of the block copolymers. As shown in Figure 2, obvious GPC MW increases were seen while the peaks remained monomodal. More convincing evidence for the formation of the block polypeptide comes from P(γ -benzyl-L-glutamate-*b*-alanine) [P(BLG-*b*-ALA)]. Polyalanine (PALA) is a polypeptide hardly soluble in common organic solvents. With a certain length of PALA segments relative to PBLG (≥ 8.4 wt %), P(BLG-*b*-ALA) becomes insoluble.⁴⁰ After adding ALA NCA into a completed $Y(BH_4)_3(THF)_3$ -catalyzed PBLG polymerization mixture, the block copolymer P(BLG-*b*-ALA) precipitated as expected. The isolated precipitate was suspended in THF, a good solvent for PBLG, and sonicated for 40 min to remove the possible homopolymers of PBLG. The THF-insoluble polymer was analyzed by 1H NMR [Fig. 1(C)]. Both peaks related to PBLG and PALA segments were resolved and identified, indicating a truly block copolymer was produced. After evaporation, no residue was left in the THF-soluble part indicating that all of the PBLG chain ends initiated the ALA NCA. Random copolymer of BLG NCA and BLL NCA was also prepared by $Y(BH_4)_3(THF)_3$ (run 4 in Table 2). The 1H NMR of the copolypeptide showed the presence of both components [Fig. 1(B)], and the calculated molar ratio of BLG to BLL units was very close to the feed ratio. GPC trace [Fig. 2(C)] exhibited a mono-modal peak with a narrow MWD of 1.07. Figure 3 summarized the DSC curves of block and random copolymers as well as homopolymers. A small liquid crystalline phase transition peak at 109 °C (T_{LC}) was observed for PBLG homopolymer. This transition which was irreversible and only occurred during the first heating run was attributed to an irreversible change from a 7/2 to a 18/5 α -helical conformation of PBLG.^{41,42} At higher temperature, no other transition was observed until its degradation.⁴² Block poly-

mer [P(BLG-*b*-BLL)] also exhibited the liquid crystalline phase transition at a slightly lower temperature (T_{LC} = 102 °C) with a smaller enthalpic change than PBLG homopolymer. This is because the α -helical conformation of PBLG segments was partially affected by PBLL and the liquid crystalline phase transition process occurred at a lower temperature. As expected, no liquid crystalline phase transition was observed for the random copolymer P(BLG-*co*-BLL), suggesting the α -helical conformation of PBLG was disrupted due to the random distribution of PBLL segments.

Mechanistic Aspects

ALA NCA instead of BLG NCA has been selected in mechanistic study due to the following three reasons. First, PALA has a simple and characteristic chemical structure. Thus, well-resolved NMR signals are expected. Second, the side reaction between the amino end group and the ester group of the last amino acid segment which is well known in BLG NCA polymerization⁴³ is absent in ALA NCA polymerization. Third, PALA precipitates during the polymerization process, resulting in low-MW polypeptide which is convenient for MALDI-TOF MS and NMR analyses.

Initiation Process of Polymerization of ALA NCA by $Y(BH_4)_3(THF)_3$

Upon reaction of the first three ALA NCA molecules with $Y(BH_4)_3(THF)_3$, all possible products are outlined in Scheme 1 corresponding to the reactions at four reactive sites of a NCA molecule. First, the $Y(BH_4)_3(THF)_3$ may initiate a nucleophilic attack at the 2-CO group of ALA NCA, leading to a borane-(S)-2-formamidopropionate which either loses the borane molecule immediately forming the yttrium (S)-2-formamidopropionate (Product I) or is reduced by borane forming the yttrium (S)-2-methylamidopropionate (Product II). However, it is need to note that this process is quite less possible for the reason that 2-CO is less reactive compared with 5-CO as reported by Kricheldorf.⁹ Second, a deprotonation could occur at the 3-NH position which is typical in the presence of strong bases.⁹ The formed *N*-yttriumlated ALA NCA could be subject to a fast rearrangement resulting in an yttrium α -isocyanato carboxylate (Product III). This is well known for NCA anions and transition metallated NCAs.⁹ Third, deprotonation of 4-CH might be taken into account although this initiation step is less favorable due to the

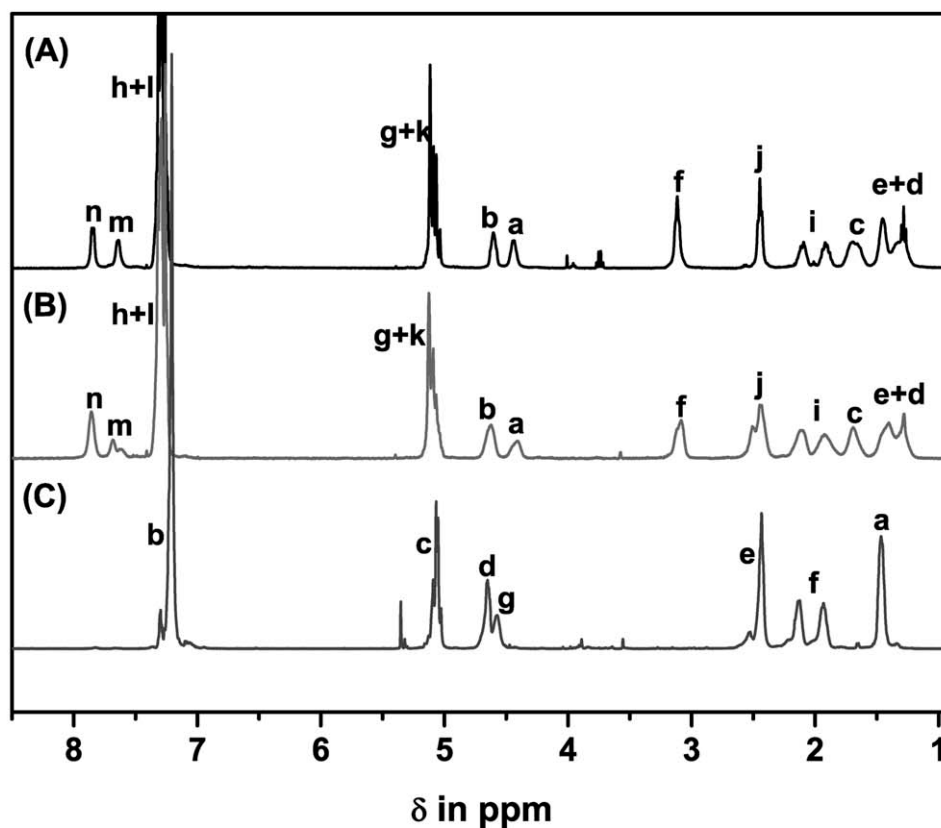
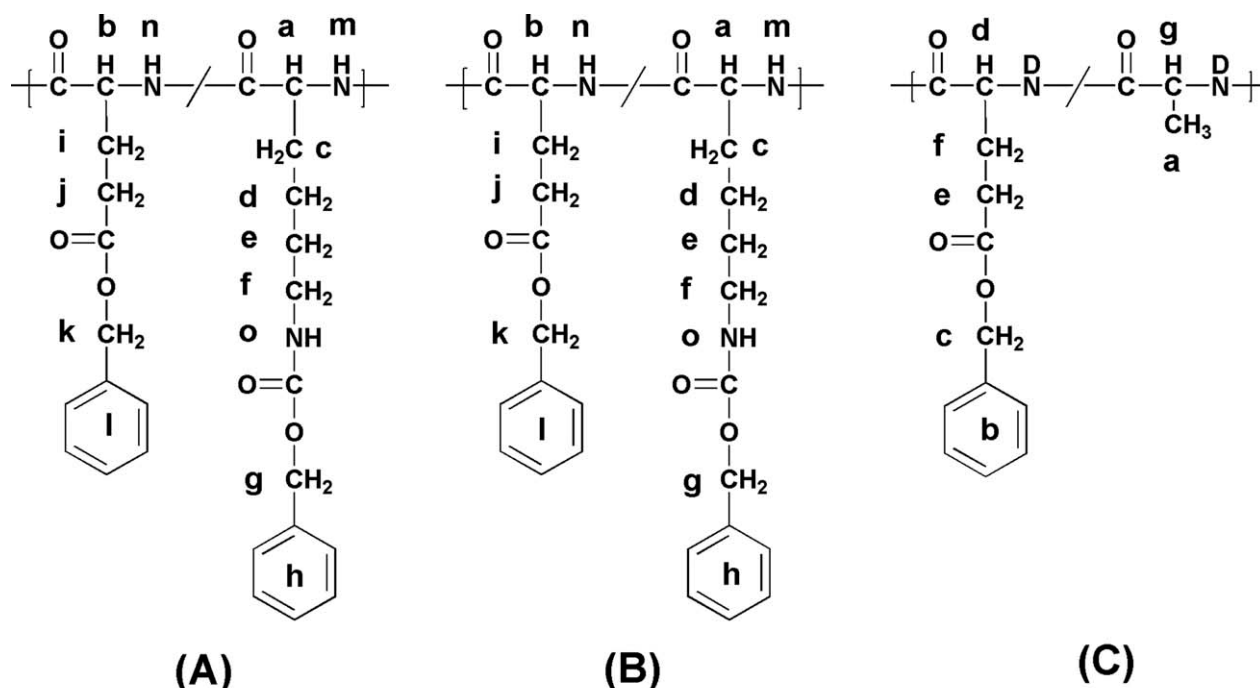


FIGURE 1 ^1H NMR spectra of P(BLG-*b*-BLL) (A) in $\text{CDCl}_3/\text{CF}_3\text{COOH}$ (run 2 in Table 2), P(BLG-*co*-BLL) (B) in $\text{CDCl}_3/\text{CF}_3\text{COOH}$ (run 4 in Table 2), and P(BLG-*b*-ALA) (C) in CF_3COOD (run 3 in Table 2).

lower acidity of the 4-proton. However, it has been shown that L-NCAs may undergo racemization in the presence of strong base⁹ indicating some acidity of the 4-proton. After

deprotonation of 4-CH, if possible, the C-yttriumlated ALA NCA might rearrange into an yttrium ketenyl carbamate (Product IV). Last, nucleophilic attack at the 5-CO is also a

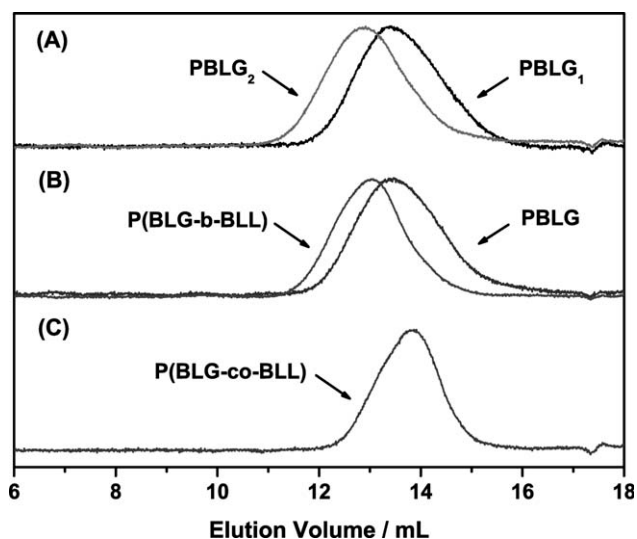


FIGURE 2 GPC traces of PBLG (A) (run 1 in Table 2), P(BLG-*b*-BLL) (B) (run 2 in Table 2), and P(BLG-*co*-BLL) (C) (Run 4 in Table 2), determined in DMF containing 0.1 mol/L LiBr at 60 °C.

potential reaction pathway (RP), after which the resulting intermediate $[-Y\{OC(O)NHCH(CH_3)C(O)HBH_3\}]$ is immediately reduced by the adjacent HBH_3 group forming the corresponding yttrium ALA carbamate derivative $[-Y\{OC(O)NHCH(CH_3)CH_2(OBH_2)\}]$ (Product V). This reduction by the HBH_3 group has been well studied in the polymerization of ϵ -caprolactone catalyzed by $Ln(BH_4)_3(THF)_3$.^{29–31} Alternatively, BH_3 could be lost by forming $[-Y\{OC(O)NHCH(CH_3)CHO\}]$ (Product VI). To understand the initiation mechanism of the polymerization and to determine which kinds of the compounds are initially formed, we performed the reaction of ALA NCA with equivalent $Y(BH_4)_3(THF)_3$ and analyzed the products by ESI-MS, FT-IR, and ^{13}C NMR.

The reaction mixture of ALA NCA with one equivalent of $Y(BH_4)_3(THF)_3$ was dissolved in anhydrous DMSO and analyzed by ESI-MS (Fig. 4) with minimum exposure to air. Major peaks were identified corresponding to structures III and V'. Product III results from the reaction at the 3-NH of ALA NCA as shown in Scheme 1. Product V' is a trimer of PALA formed by addition of two ALA to compound V (Scheme 1). During negative ionization in ESI-MS, the initially formed compound V'' releases a CO_2 molecule forming into the Product V', a well-documented process.⁹ These results indicate that both 3-NH and 5-CO of ALA NCA are involved in the initiation process and rules out the other potential reactions shown in Scheme 1. Because of the higher energy barrier of deprotonation at 3-NH relative to nucleophilic attack at the 5-CO of an ALA NCA,⁹ the ring-opening process at the 5-CO group is faster than the deprotonation at 3-NH resulting in the competitive products of ALA trimer V' and unimer of III.

Formation of III and V' is further supported by FT-IR analyses (Fig. 5). Two characteristic stretching vibrations of ALA NCA anhydride can be distinguished in Figure 5(A) with the frequency at 1839 cm^{-1} assigned to 5-CO and 1778 cm^{-1} to

2-CO. The reduced frequency of 2-CO compared with 5-CO is caused by the nitrogen electron pair delocalized on to the 5-CO. This assignment has been demonstrated by Kricheldorf.⁹ The spectrum of $Y(BH_4)_3(THF)_3$ [Fig. 5(B)] displays three bands corresponding to the $\nu(B-H_{\text{terminal}})$ ($2450\text{--}2430\text{ cm}^{-1}$), $\nu(B-H_{\text{bridging}})$ ($2230\text{--}2110\text{ cm}^{-1}$), and $\delta(B-H)$ (1119 cm^{-1}), as found in the literature for rare earth metallic borohydride complexes of La, Nd, and Sm.³⁰ Figure 5(C) shows the FT-IR spectrum of the reaction with 1 equiv of the yttrium complex. The disappearance of the absorption bands corresponding to HBH_3 groups indicates the cleavage of the B–H bonds in $Y(BH_4)_3(THF)_3$ during the initiation process. The 2-CO band of ALA NCA ring shifts toward lower frequencies (1747 cm^{-1}) compared with monomer ALA NCA [Fig. 5(A)]. It is attributed to the formation of the *N*-yttriumated ALA NCA with the increasing electronegativity of the nitrogen atom after being yttriumated. The *N*-yttriumated ALA NCA undergoes a rearrangement into yttrium α -isocyanato carboxylate according to the detection of stretching vibrations of isocyanate group⁴⁴ (2391 cm^{-1}) and yttrium carboxylate (1580 cm^{-1}) group. Evidence of V' is provided by the CO band of the amide group located at 1648 cm^{-1} together with the CO band of yttrium carbamate group residing at 1580 cm^{-1} which is overlapped with yttrium carboxylate.

CF_3COOD was used as the solvent for a better NMR resolution. The ^{13}C NMR spectrum of the carbonyl groups of the acidolysis product is shown in Figure 6 with all ^{13}C signals of carbonyl groups of III_F and V'_F well resolved. Both Products III and V' react with CF_3COOD yielding corresponding Products III_F and V'_F, respectively. The chemical shifts of the carbonyl groups of III_F are assigned according to the model compound hexyl isocyanate (Supporting Information Fig. S1).

The above results indicate that only 3-NH and 5-CO are involved in the initiation step. We further used the equivalent reaction product to initiate ROP of BLG NCA. As expected, it polymerized BLG NCA in quantitative yield (95%). The fragment originating from Product V' is clearly identified in 1H NMR spectrum of the produced PBLG

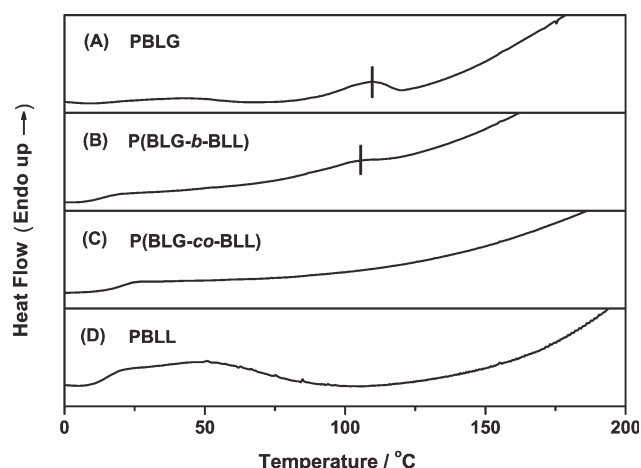
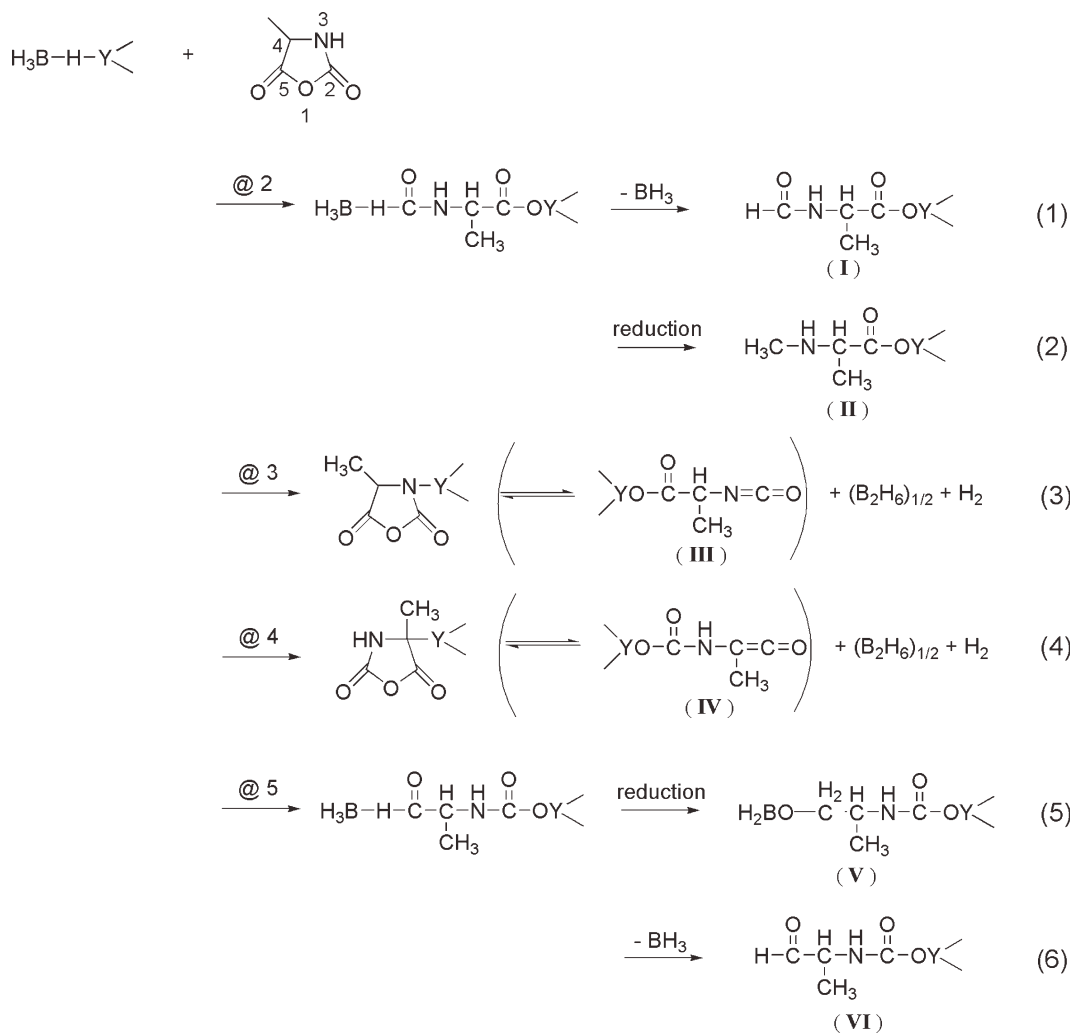


FIGURE 3 DSC thermograms of PBLG (A), P(BLG-*b*-BLL) (B), P(BLG-*co*-BLL) (C), and PBL (D).



SCHEME 1 Possible mechanisms for the initiation process of ALA NCA polymerization catalyzed by $Y(BH_4)_3(THF)_3$.

(Fig. 7), implying compound V' is the active initiation species responsible for further chain growth. The *N*-yttriumlated ALA NCA (Product III) which is also expected to initiate a polymerization will be discussed below.

Propagation Process of the Polymerization of ALA NCA in the Presence of $Y(BH_4)_3(THF)_3$

It is well known that two different reaction mechanisms are adopted during ROP of NCA, that is, the normal amine mechanism (NAM) and the activated monomer mechanism (AMM), depending on the relative nucleophilicity and basicity of the initiator. Identification of the end groups can distinguish the mechanism. Primary amine, hexylamine for example, a well-known catalyst for NAM, produces a polypeptide chain containing a hexyl end and amino end groups,²⁴ whereas *N*-ethyl-diisopropylamine, a tertiary amine, initiating ROP via AMM, creates a chain with an amino group at one end and a carboxyl group at the other resulting from the attack of H_2O to the *N*-acyl-NCA end group.²⁶

To investigate the mechanism, ALA NCA was polymerized by $Y(BH_4)_3(THF)_3$ at room temperature for 3 days with the

molar ratio of monomer to catalyst of 30. The MALDI-TOF MS result of the produced PALA is shown in Figure 8. Two populations of polymers corresponding to the chemical structures of A and B are resolved. All polymers contain an amino group at one end and either a hydroxyl (structure A) or carboxyl group (structure B) at the other. The adjacent peaks of each population have the margin of 71 Da corresponding to an ALA repeating unit.

The end groups of PALA are further demonstrated by NMR. Thus, 1H NMR, ^{13}C NMR, 1H - 1H COSY, and 1H - ^{13}C HMQC spectra of PALA are illustrated in Figures 9 and 10 and Supporting Information S2 and S3, respectively, with full assignments. NMR analyses of PALA reveal three distinct chain ends, that is, carboxyl groups, amino groups, and hydroxyl groups. Among the three end groups, hydroxyl end group ($HOCH_2CH(CH_3)NH-$) is well resolved and the whole set signals (Hc, Hf, Hg₁, Hg₂, Hc-Hf, Hc-Hg₁, Hc-Cc, Hf-Cf, Hg₁-Cg, Hg₂-Cg, Cc, Cf, and Cg) can be observed unambiguously.⁴⁵ This set signals are due to $Ln(BH_4)_3(THF)_3$ -catalyzed PALA as they are absent in water- or tertiary amine-catalyzed PALA [Fig. 9(B,C)]. The signals of carboxyl end group and

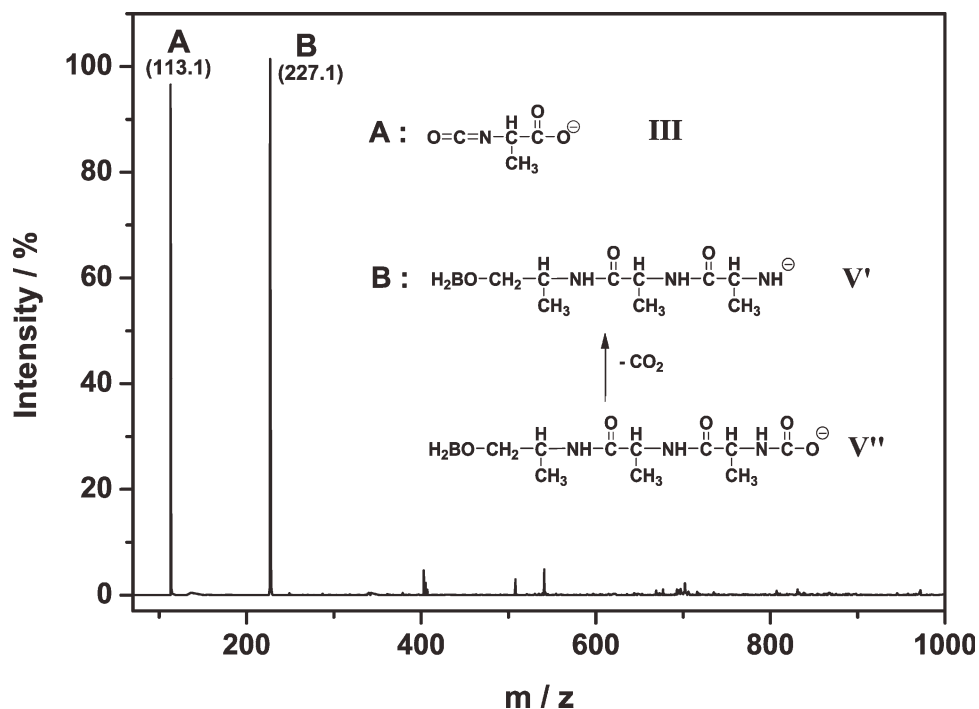


FIGURE 4 ESI-MS spectrum (negative ionization) of the reaction mixture of ALA NCA and equivalent $Y(BH_4)_3(THF)_3$.

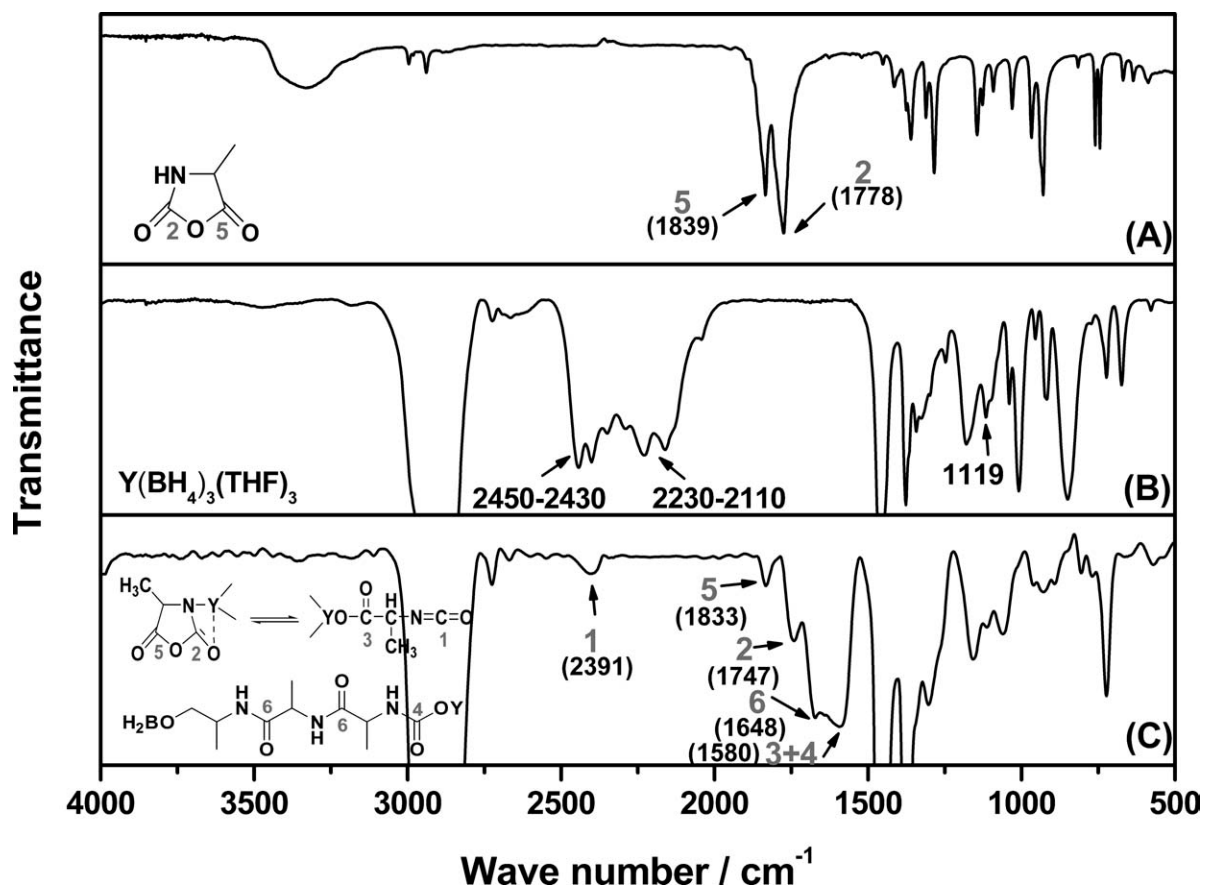


FIGURE 5 FT-IR spectra of ALA NCA (A), $Y(BH_4)_3(THF)_3$ (B), and the reaction mixture (C) of ALA NCA with equivalent $Y(BH_4)_3(THF)_3$.

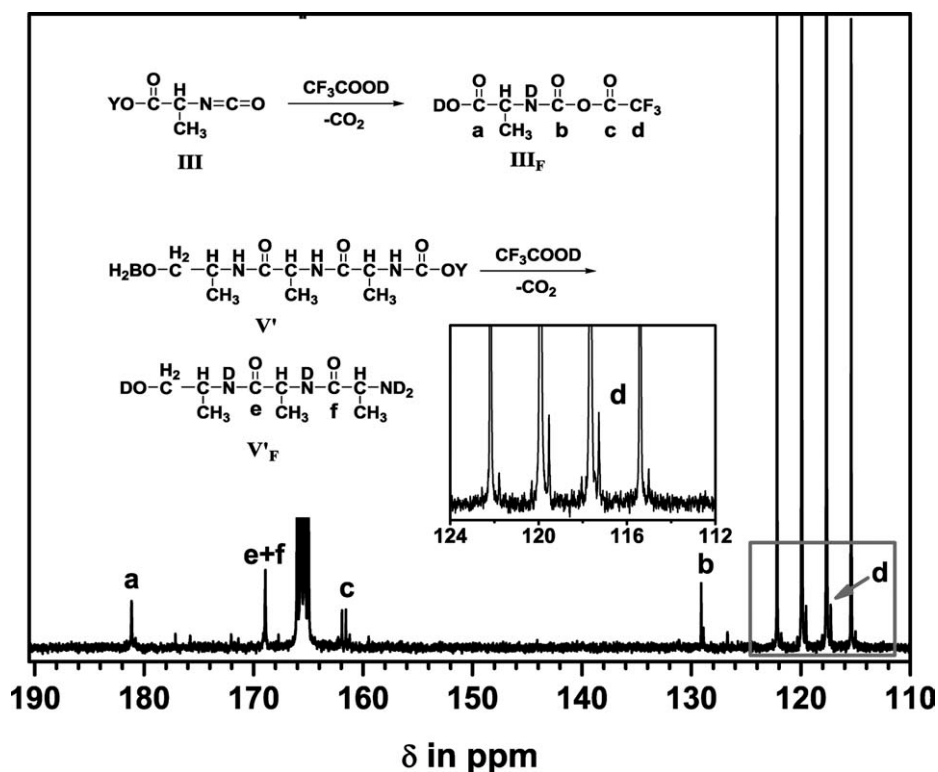


FIGURE 6 Partial ^{13}C NMR spectrum of the product of ALA NCA with equivalent $\text{Y}(\text{BH}_4)_3(\text{THF})_3$ using CF_3COOD as the solvent.

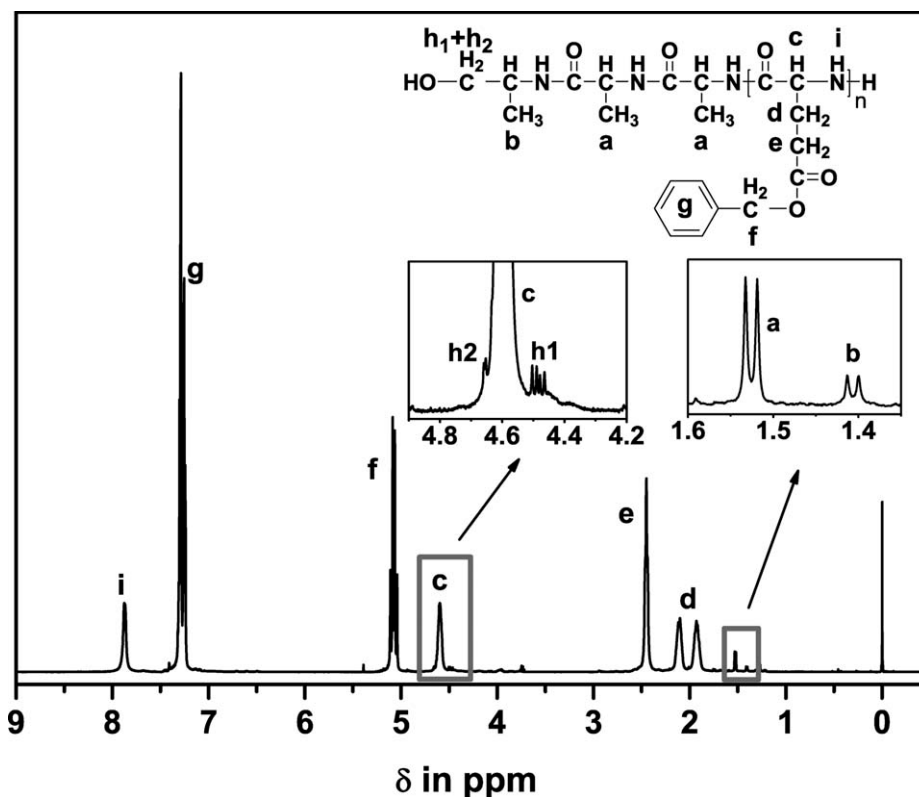


FIGURE 7 ^1H NMR spectrum of PBLG initiated by the product of ALA NCA reacting with equivalent $\text{Y}(\text{BH}_4)_3(\text{THF})_3$. Reaction conditions: $[\text{BLG NCA}] = 1.0 \text{ mol/L}$, $m(\text{BLG NCA})/m(\text{equivalent reaction product}) = 800/11.6 \text{ mg}$, THF, 25°C , 3 days.

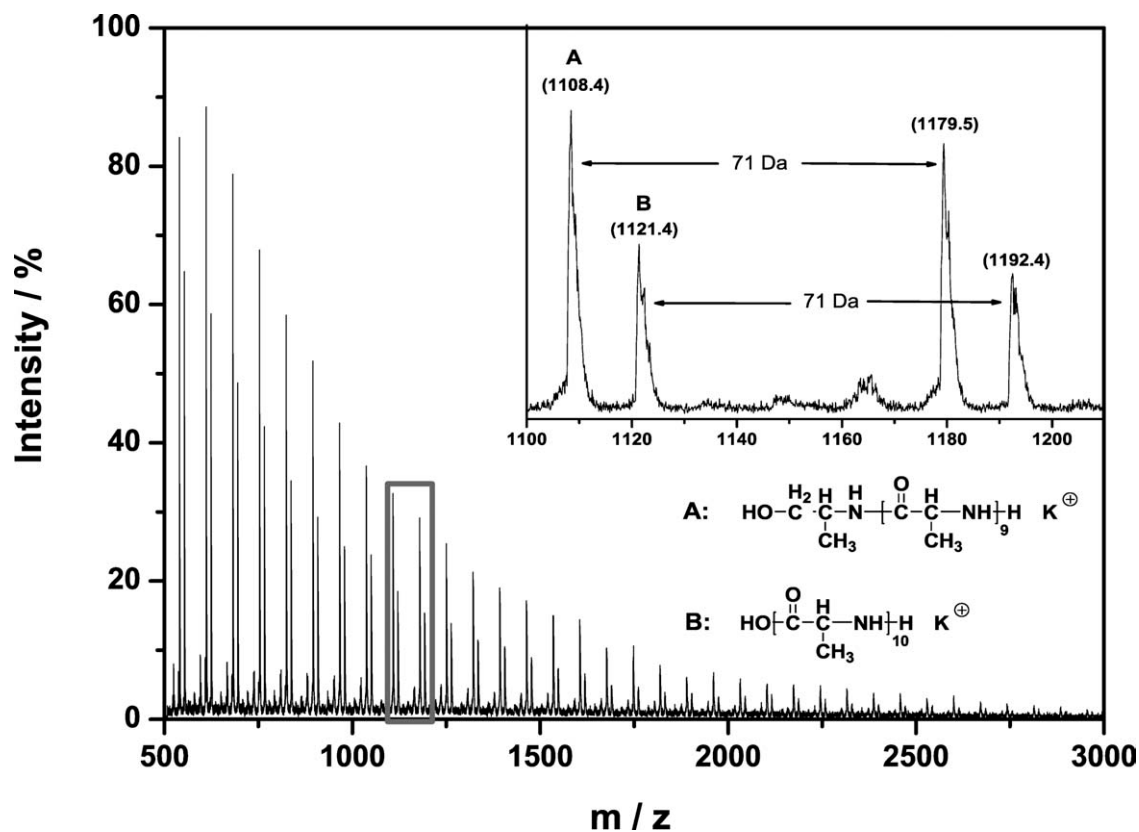


FIGURE 8 MALDI-TOF mass spectrum (K^+ doping) of PALA catalyzed by $\text{Y}(\text{BH}_4)_3(\text{THF})_3$ at 25°C .

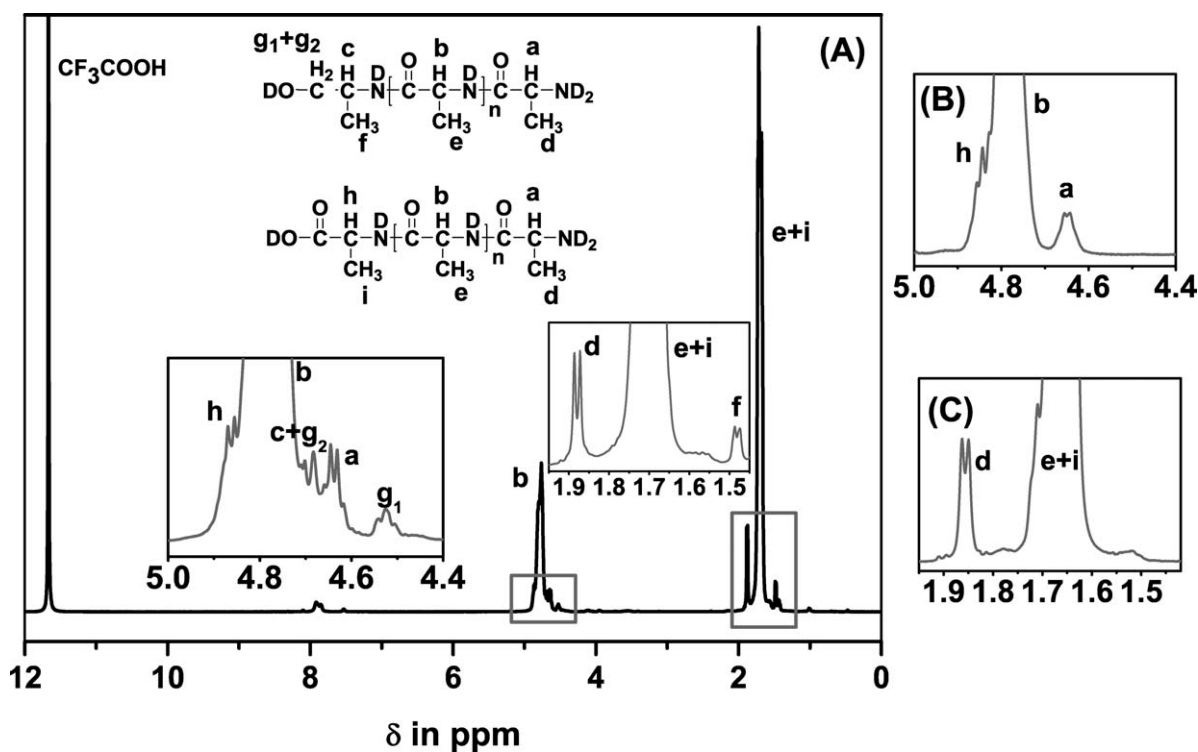


FIGURE 9 ^1H NMR spectra of PALA catalyzed by $\text{Y}(\text{BH}_4)_3(\text{THF})_3$ (A) and PALA by H_2O (B and C) for comparison. CF_3COOD is used as the solvent.

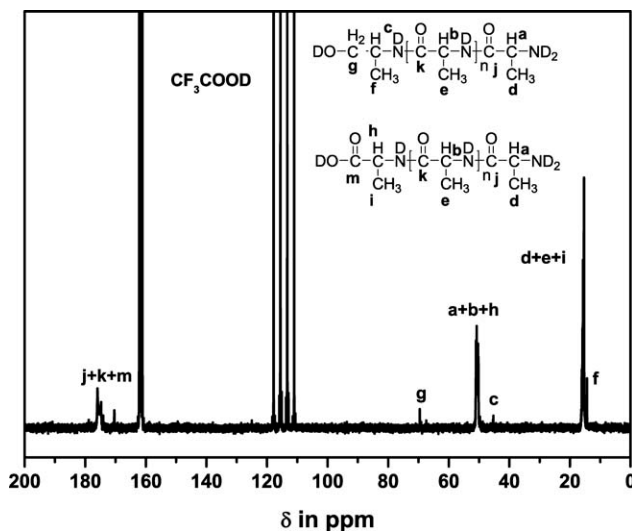


FIGURE 10 ^{13}C NMR spectrum of PALA catalyzed by $\text{Y}(\text{BH}_4)_3(\text{THF})_3$. CF_3COOD is used as the solvent.

amino end group are partially overlapped with the main chain signals in ^1H and ^{13}C spectra and can be resolved by means of ^1H - ^1H COSY (Supporting Information Fig. S2) and ^1H - ^{13}C HMQC (Supporting Information Fig. S3) spectra.⁴⁶

From the results above, two different RPs take place concurrently during the ROP of NCA catalyzed by $\text{Ln}(\text{BH}_4)_3(\text{THF})_3$ as summarized in Scheme 2. RP-1 and RP-2 are proposed to explain the formation of the α -hydroxyl- ω -aminotelechelic PALA chain and the α -carboxylic- ω -aminotelechelic PALA chain, respectively. In RP-1 (Scheme 2), after attacking at 5-CO by $\text{Ln}(\text{BH}_4)_3(\text{THF})_3$, the NCA ring opens and inserts into the $\text{Ln}-\text{HBH}_3$ bond resulting an intermediate $[-\text{Ln}\{\text{OC}(\text{O})\text{NHCH}(\text{CH}_3)\text{C}(\text{O})\text{HBH}_3\}]$ (Product VII) in which the HBH_3 group immediately reacts with the α -carbonyl group to form the corresponding rare earth ALA carbamate derivative $-\text{Ln}\{\text{OC}(\text{O})\text{NHCH}(\text{CH}_3)\text{CH}_2(\text{OBH}_2)\}$ (V). Similar reductive ability of the borohydride ligand in $\text{Ln}(\text{BH}_4)_3(\text{THF})_3$ has been well studied in lactone polymerization by Guillaume and co-workers.^{29,31} Polymerization of ALA NCA by V then proceeds through the rare earth carbamate attacking at the 5-CO of the monomer resulting in the C5-O1 acyl-oxygen bond cleavage followed by the release of a CO_2 molecule. The reaction is quenched by H_2O resulting in the hydrolysis of the active $\text{Ln}-\text{OCONH}$ bond and release of CO_2 , generating the amino chain end. Meanwhile, the other end of the polymer chain capped with a hydroxyl group results from the hydrolysis of the $-\text{NHCH}(\text{CH}_3)\text{CH}_2(\text{OBH}_2)$ chain end. As there are no termination steps, a living polymerization is expected in the case of RP-1. The competing RP-2 process, however, is a combination of chain propagation and step-growth processes. A deprotonation step at 3-NH by $\text{Ln}(\text{BH}_4)_3(\text{THF})_3$ happens forming a N-rare earth metallated NCA (Product VIII) accompanied with the $\text{BH}_3\cdot\text{THF}$ adduct and a molecule of hydrogen gas. Attack at the 5-CO of ALA NCA by complex VIII leads to a dimer (Product IX) containing a highly electrophilic N-acyl NCA end group and a

nucleophilic carbamate group. Further, chain growth can proceed either via RP-1 at the rare earth carbamate end or via nucleophilic attack at the 5-CO group of the N-acyl NCA end of IX by another N-rare earth metallated NCA (VIII) or rare earth carbamate end. PALA with a N-acyl NCA end group and a rare earth carbamate end group is formed after complete consumption of NCA monomers. The carboxylic end group is generated by the addition of H_2O which attacks at the 5-CO of N-acyl NCA end group followed by decarboxylation. The amino end group results from the hydrolysis of the rare earth carbamate end group. It is worth mentioning that growing chains can switch back and forth between the RP-1 and RP-2 processes during the polymerization. The active rare earth carbamate chain end of RP-1 can attack at the active N-acyl NCA end group of RP-2 or a N-rare earth metallated NCA, whereas the active rare earth carbamate chain end of RP-2 can also proceed a polymerization through a normal chain propagation of RP-1. Thus, GPC traces exhibit a mono-modal peak though two different RPs take place at the same time and the obtained M_n s are higher than theoretical ones (Table 1).

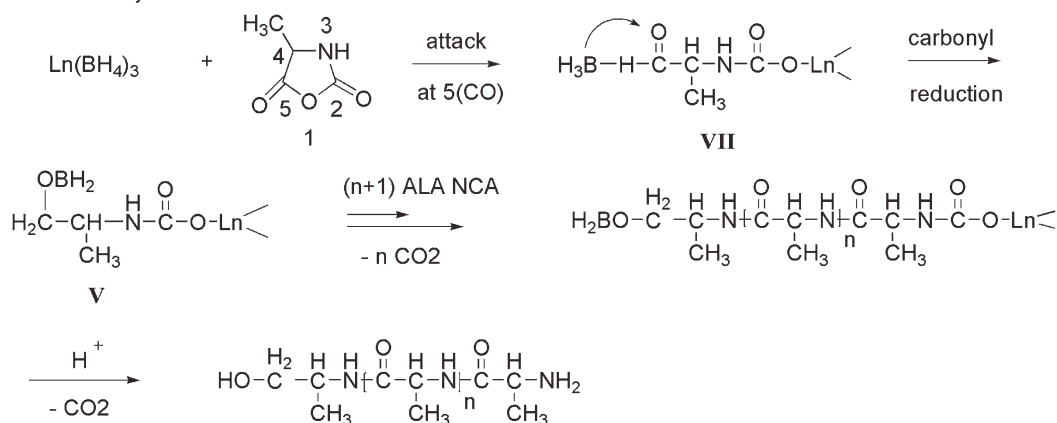
Synthesis of α -Hydroxyl- ω -Aminotelechelic Polypeptide

Compared with conventional α -carboxylic- ω -amino-protein, α -hydroxyl- ω -aminotelechelic polypeptide may have different self-assembly behaviors and salting-out effects. Furthermore, the hydroxyl end group provides a potential site for drug conjugation, facilitating its use as drug/gene carrier or in other biomedical applications. However, its preparation by reduction from the corresponding α -carboxylic- ω -aminotelechelic polypeptide is prone to either over-reduction or incomplete reduction by the common reducing agents, namely LiAlH_4 or $\text{H}_2/\text{Pd-C}$ and NaBH_4 (data not shown). Therefore, the synthesis of a pure α -hydroxyl- ω -aminotelechelic polypeptide is of great interest. It is well known that nucleophilic attack at 5-CO is a fast initiation step while deprotonation at 3-NH is a much slower process requiring a higher activation energy.⁹ Hence, when the polymerization was performed at 0°C to suppress RP-2, we demonstrated that only RP-1 took place. The MALDI-TOF MS of the product is shown in Figure 11. Only one population corresponding to the structure A is resolved. In ^1H NMR (Supporting Information Fig. S4), the proton of the methine linked to carboxylic group disappears while the set of the hydroxyl group is still resolved. The results indicate that a lowering reaction temperature can effectively avoid the deprotonation step, producing pure telechelic polypeptides with amino and hydroxyl end groups.

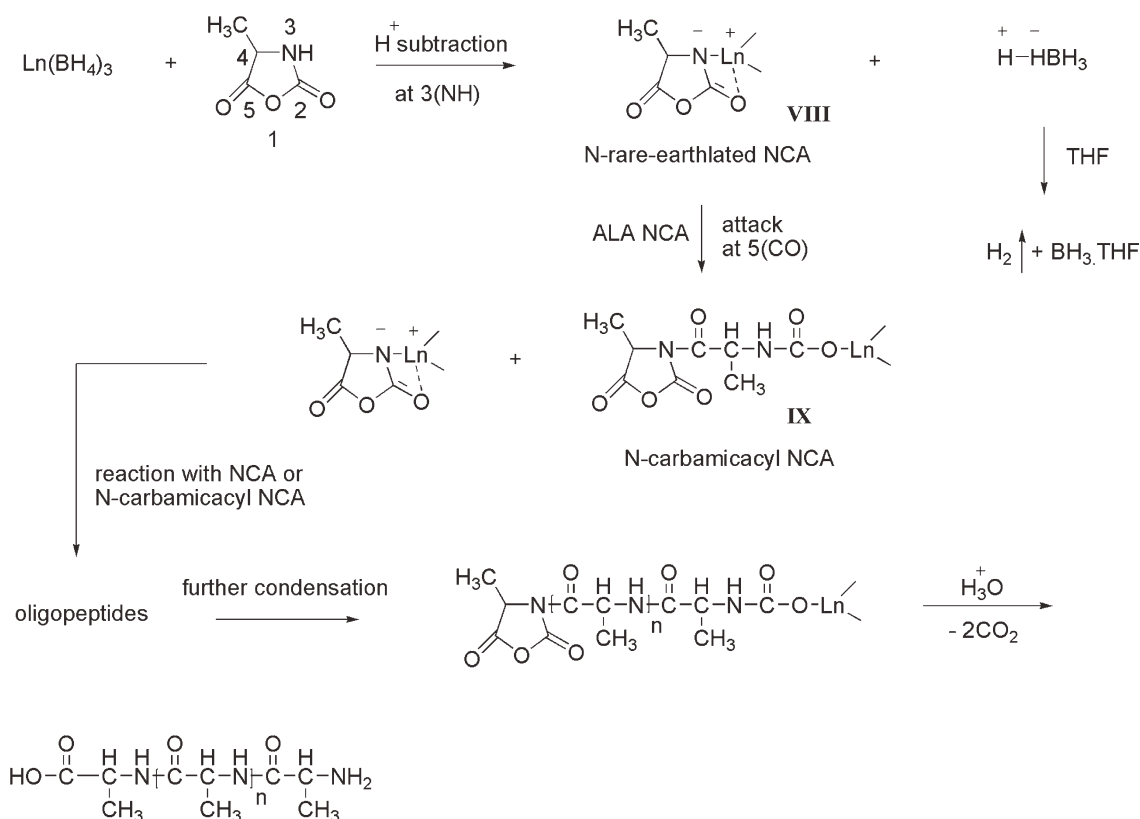
CONCLUSIONS

Rare earth borohydride complexes $\text{Ln}(\text{BH}_4)_3(\text{THF})_3$ ($\text{Ln} = \text{Sc}, \text{Y}, \text{La}, \text{and Dy}$) have been applied to catalyze the ROP of BLG NCA for the first time. The catalysts exhibit high activities producing polypeptides in quantitative yields. The MWs of the PBLG can be controlled by the molar ratios of monomer to catalyst, and the MWDs are relatively narrow (1.16–1.65) depending on the rare earth metals and reaction temperatures. Block copolypeptides have been facily synthesized by

Reaction Pathway 1:



Reaction Pathway 2:



SCHEME 2 Mechanism for the ROP of ALA NCA catalyzed by $\text{Ln}(\text{BH}_4)_3(\text{THF})_3$.

sequential addition of two monomers. Random copolypeptide with MWD as narrow as 1.07 has been produced. In mechanic studies, we have found two active species, that is, an yttrium ALA carbamate derivative (V) and a *N*-yttrium-lated ALA NCA (VIII) which are derived from the reactions of 5-CO and 3-NH of ALA NCA with $\text{Y}(\text{BH}_4)_3(\text{THF})_3$, respectively, initiate the polymerizations simultaneously, leading to the α -hydroxyl- ω -aminotelechelic polypeptides and α -carbox-

yl- ω -aminotelechelic ones. Lowering the reaction temperature to 0 °C can effectively suppress the deprotonation of 3-NH, producing a pure α -hydroxyl- ω -aminotelechelic polypeptide. This study highlights that it provides an insight into the mechanism of NCA polymerization catalyzed by organometallic catalysts. The improved versatility of such rare earth tris(-borohydride) compounds, relative to other catalysts, lies in their ability to generate an unprecedented α -hydroxyl- ω -

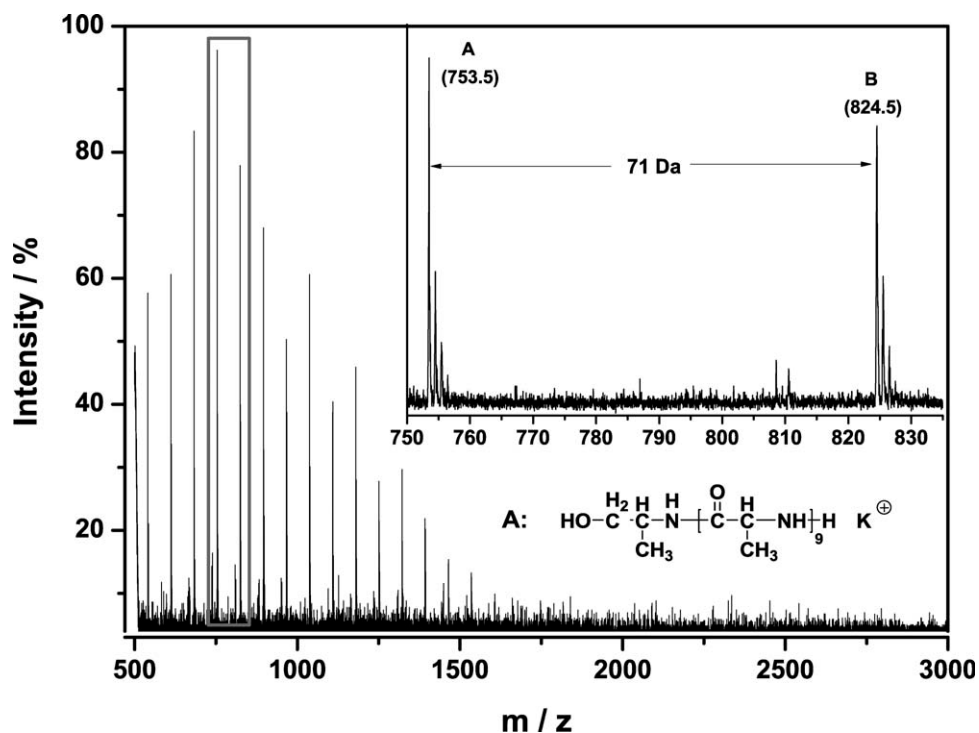


FIGURE 11 MALDI-TOF mass spectrum (K^+ doping) of PALA catalyzed by $Y(BH_4)_3(THF)_3$ at $0^\circ C$.

aminotelechelic polypeptide which may be used as an improved biomaterial or an effective macroinitiator to afford a polyester/polypeptide conjugate.

ACKNOWLEDGMENTS

H. R. Kricheldorf is warmly acknowledged for his helpful discussions. The authors are grateful to the National Natural Science Foundation of China (21174122), the Special Funds for Major Basic Research Projects (G2011CB606001), the Zhejiang Provincial Natural Science Foundation of China (Y4110115), and the Fundamental Research Funds for the Central Universities (2011QNA4025).

REFERENCES AND NOTES

- Zhang, Z.; Chen, L.; Deng, M. X.; Bai, Y. Y.; Chen, X. S.; Jing, X. B. *J. Polym. Sci. Part A: Polym. Chem.* **2011**, *49*, 2941–2951.
- Zeng, X.; Zhang, Y.; Wu, Z.; Lundberg, P.; Malkoch, M.; Nyström, A. M. *J. Polym. Sci. Part A: Polym. Chem.* **2012**, *50*, 280–288.
- Tang, H.; Lee, C.; Zhang, D. *J. Polym. Sci. Part A: Polym. Chem.* **2011**, *49*, 3228–3238.
- Lin, Y. C.; Kuo, S. W. *J. Polym. Sci. Part A: Polym. Chem.* **2011**, *49*, 2127–2137.
- Deming, T. J. *Adv. Mater.* **1997**, *9*, 299–311.
- Kricheldorf, H. R. *Angew. Chem. Int. Ed. Engl.* **2006**, *45*, 5752–5784.
- Hadjichristidis, N.; Latrou, H.; Pitsikalis, M.; Sakellariou, G. *Chem. Rev.* **2009**, *109*, 5528–5578.
- Zhang, X. W.; Odon, M.; Giani, O.; Monge, S.; Robin, J. J. *Macromolecules* **2010**, *43*, 2654–2656.
- Kricheldorf, H. R. *α -Aminoacid-N-Carboxy-Anhydrides and Related Heterocycles*; Springer-Verlag: Berlin, **1987**; pp 1–213.

- Deming, T. J. *J. Am. Chem. Soc.* **1997**, *119*, 2759–2760.
- Lu, H.; Cheng, J. *J. Am. Chem. Soc.* **2008**, *130*, 12562–12563.
- Deming, T. J. *Nature* **1997**, *390*, 386–389.
- Deming, T. J. *J. Am. Chem. Soc.* **1998**, *120*, 4240–4241.
- Lu, H.; Cheng, J. *J. Am. Chem. Soc.* **2007**, *129*, 14114–14115.
- Lu, H.; Wang, J.; Lin, Y.; Cheng, J. *J. Am. Chem. Soc.* **2009**, *131*, 13582–13583.
- Aliferis, T.; Latrou, H.; Hadjichristidis, N. *Biomacromolecules* **2004**, *5*, 1653–1656.
- Karatzas, A.; Latrou, H.; Hadjichristidis, N.; Inoue, K.; Sugiyama, K.; Hirao, A. *Biomacromolecules* **2008**, *9*, 2072–2080.
- Aliferis, T.; Latrou, H.; Hadjichristidis, N. *J. Polym. Sci. Part A: Polym. Chem.* **2005**, *43*, 4670–4673.
- Cottet, H.; Vayaboury, W.; Kirby, D.; Giani, O.; Taillades, J.; Schué, F. *Anal. Chem.* **2003**, *75*, 5554–5560.
- Vayaboury, W.; Giani, O.; Cottet, H.; Deratani, A.; Schué, F. *Macromol. Rapid Commun.* **2004**, *25*, 1221–1224.
- Habraken, G. J. M.; Peeters, M.; Dietz, C. H. J. T.; Koning, C. E.; Heise, A. *Polym. Chem.* **2010**, *1*, 514–524.
- Habraken, G. J. M.; Wilsens, K. H. R. M.; Koning, C. E.; Heise, A. *Polym. Chem.* **2011**, *2*, 1322–1330.
- Dimitrov, I.; Schlaad, H. *Chem. Commun.* **2003**, *23*, 2944–2945.
- Kricheldorf, H. R.; Lossow, C. V.; Schwarz, G. *Macromol. Chem. Phys.* **2004**, *205*, 918–924.
- Kricheldorf, H. R.; Lossow, C. V.; Schwarz, G. *Macromol. Chem. Phys.* **2005**, *206*, 282–290.
- Kricheldorf, H. R.; Lossow, C. V.; Schwarz, G. *J. Polym. Sci. Part A: Polym. Chem.* **2006**, *44*, 4680–4695.
- Pickel, D. L.; Politakos, N.; Avgeropoulos, A.; Messman, J. M. *Macromolecules* **2009**, *42*, 7781–7787.
- Ling, J.; Huang, Y. *Macromol. Chem. Phys.* **2010**, *211*, 1708–1711.

- 29** Guillaume, S. M.; Schappacher, M.; Soum, A. *Macromolecules* **2003**, *36*, 54–60.
- 30** Palard, I.; Soum, A.; Guillaume, S. M. *Macromolecules* **2005**, *38*, 6888–6894.
- 31** Palard, I.; Schappacher, M.; Belloncle, B.; Soum, A.; Guillaume, S. M. *Chem. Eur. J.* **2007**, *13*, 1511–1521.
- 32** Zhao, W.; Cui, D.; Liu, X.; Chen, X. *Macromolecules* **2010**, *43*, 6678–6684.
- 33** Gao, W.; Cui, D.; Liu, X.; Zhang, Y.; Mu, Y. *Organometallics* **2008**, *27*, 5889–5893.
- 34** Ling, J.; Shen, Z.; Huang, Q. *Macromolecules* **2001**, *34*, 7613–7616.
- 35** Shen, Y.; Shen, Z.; Zhang, Y.; Yao, K. *Macromolecules* **1996**, *29*, 8289–8295.
- 36** Ling, J.; Zhang, Y. F.; Shen, Z. Q. *Chin. Chem. Lett.* **2001**, *12*, 41–42.
- 37** Hu, X.; Wu, J.; Xu, Z.; Feng, L. *Chin. J. Polym. Sci.* **2000**, *18*, 369–372.
- 38** Wu, G.; Sun, W.; Shen, Z. *React. Funct. Polym.* **2008**, *68*, 822–830.
- 39** Blout, E. R.; Karlson, R. H. *J. Am. Chem. Soc.* **1956**, *78*, 941–946.
- 40** Gitsas, A.; Floudas, G.; Mondeshki, M.; Spiess, H. W.; Aliferis, T.; Latrou, H.; Hadjichristidis, N. *Macromolecules* **2008**, *41*, 8072–8080.
- 41** Lecommandoux, S.; Achard, M. F.; Langenwalter, J. F.; Klok, H. A. *Macromolecules* **2001**, *34*, 9100–9111.
- 42** Caillol, S.; Lecommandoux, S.; Mingotaud, A. F.; Schappacher, M.; Soum, A.; Bryson, N.; Meyrueix, R. *Macromolecules* **2003**, *36*, 1118–1124.
- 43** Fontaine, L.; Ménard, L.; Brosse, J. C.; Sennyey, G.; Senet, J. P. *React. Funct. Polym.* **2001**, *47*, 11–21.
- 44** We proved this band did not arise from CO₂ absorption as this peak could be resolved after CO₂ background was subtracted.
- 45** There are two things need to mention in assigning the NMR signals. First, the methylene linked to a hydroxyl group (HOCH₂) is usually located in 3–4 ppm in CDCl₃ solvent but in the present one, the signals appear at 4.53 ppm (Hg₁) and 4.69 ppm (Hg₂). We have proved this down-field transfer phenomenon is caused by the solvent CF₃COOD. Similar end group (HOCH₂–) signal of a poly(ϵ -caprolactone) chain located originally at 3.65 ppm in CDCl₃ moves to 4.40 ppm in a mixed solvent CDCl₃/CF₃COOH (v:v = 3:1). Second, the proton signal of Hg₂ is overlapped with Hc and Hb in ¹H NMR, resulting in the difficulty to find the coupling signal Hc-Hg₂ in ¹H-¹H COSY. Fortunately, it can be clearly identified in ¹H-¹³C HMQC (Hg₁-Cg and Hg₂-Cg) proving the existence of a Hg₂ proton. The diastereotopic methylene protons of Hg₁ and Hg₂ locating at 4.53 ppm and 4.69 ppm, respectively, have a geminal coupling constant of 80 Hz.
- 46** The signal Ha in Figure 9 is assigned to the methine proton of amino end group and the signal Hh is of carboxyl end group because carboxyl group is more electron-withdrawing than amino group. The ¹H NMR spectrum of PALA methlate obtained from the reaction of imidazole end group of PALA with methanol shows the signal corresponding to the amino end while the carboxyl end signal disappears.⁴⁷
- 47** Kricheldorf, H. R.; Lossow, C. V.; Schwarz, G. *J. Polym. Sci. Part A: Polym. Chem.* **2005**, *43*, 5690–5698.